BMC Medical Imaging

RESEARCH

Open Access

CT-based delta-radiomics for predicting pathological response to neoadjuvant immunochemotherapy in esophageal squamous cell carcinoma: a multicenter study

Yuting Zheng[1,2†], Peiyuan Mei[3†], Mingliang Wang[4†], Qinyue Luo[1,2†], Hanting Li[1,2], Chengyu Ding[5], Kailu Zhang[1,2], Leqing Chen[1,2], Jin Gu[1,2], Yumin Li[1,2], Tingting Guo[1,2], Chi Zhang[3], Wenjian Yao[4], Li Wei[4*], Yongde Liao[3*], Xiaoyu Han[1,2*] and Heshui Shi[1,2*]

Abstract

Background The study aimed to investigate the predictive value of delta-radiomics derived from computed tomography (CT) for pathological complete response (pCR) to neoadjuvant immunochemotherapy (NICT) among patients with esophageal squamous cell carcinoma (ESCC), helping clinicians determine whether to modify the neoadjuvant treatment strategy, proceed to surgery, or forgo surgery altogether.

Methods A total of 140 ESCC patients from two institutions (Database 1 = 93; Database 2 = 47) who underwent NICT and surgery were retrospectively included in the study. The training set consisted of patients from Database 1, while the testing set included patients from Database 2. All patients underwent contrast-enhanced CT scans before the start of the treatment and prior to the operation. The delta-radiomics features were calculated as the relative net change of radiomics features between the two-time points. Feature selection was conducted using Pearson correlation analysis, intraclass correlation coefficients, and the fivefold cross-validation with least absolute shrinkage and selection analysis. Four models were established, comprising a clinical model, a pre-treatment radiomics model, a delta-radiomics model, and a mixed model. Area under the curve (AUC) and decision curve analysis were used to assess the performance and the clinical value of the models.

†Yuting Zheng, Peiyuan Mei, Mingliang Wang and Qinyue Luo contributed equally to this work.

*Correspondence:
Li Wei
weilihn66@163.com
Yongde Liao
liaotjxw@126.com
Xiaoyu Han
xiaoyuhan1123@163.com
Heshui Shi
heshuishi@hust.edu.cn

Full list of author information is available at the end of the article

Results Less than half of the tumors (40/140, 28.6%) showed pCR following NICT. The delta-radiomics model displayed AUC of 0.827 and 0.790 in the training and testing set for predicting pCR, which was superior to the clinical model based on age and clinical tumor node metastasis (cTNM) stage (0.758 and 0.615) and the pre-treatment radiomics model (0.787 and 0.621). Furthermore, the delta-radiomics model demonstrated a more excellent AUC value in the testing set than the mixed model (0.847 and 0.719), which integrated clinical and delta-radiomics features.

Conclusions The delta-radiomics model exhibited better diagnostic performance in preoperative prediction of pCR for NICT in ESCC patients compared to the clinical, pre-treatment radiomics, and mixed models.

Keywords Esophageal squamous cell carcinoma, Computed tomography, Delta-radiomics, Neoadjuvant immunochemotherapy, Pathological response

Background

Esophageal cancer is a widespread cancer with a high fatality rate worldwide [1, 2]. Asia has the highest incidence, where esophageal squamous cell carcinoma (ESCC) is the most common type [3, 4]. Neoadjuvant immunochemotherapy (NICT) has recently shown promising results in patients with ESCC. Emerging evidence has demonstrated that NICT can induce optimal tumor regression, have low adverse effects, limit postoperative complications, and may even provide survival benefits for patients suffering from advanced ESCC [5–7].

Pathological complete response (pCR) is regarded as a substantial therapeutic outcome of neoadjuvant treatment and a reliable surrogate indicator for assessing postoperative survival [8]. Accurate prediction of pCR is crucial for guiding treatment decisions, as not all patients benefit from NICT. Ineffective neoadjuvant therapy might lead to postponed surgery and raise the risk of unnecessary adverse events and immune-related adverse events (irAEs) manifesting as hematologic and gastrointestinal toxicity, pneumonitis, hypothyroidism, and hepatitis, among others [9]. By predicting whether patients achieve pCR after neoadjuvant therapy, it assists doctors in determining whether to modify the neoadjuvant treatment strategy, proceed to surgery or forget surgery completely. Since pCR can only be confirmed after surgery, several studies have explored clinical and radiographic parameters before surgery to predict pCR to NICT for ESCC [8, 10–12], including metabolic parameters from positron emission tomography (PET) and systemic inflammation-tumor markers. Despite their predictive value, hematological indexes can be influenced by various factors, and metabolic parameters may not represent the spatial distribution of the entire tumor. Thus, it is crucial to discover more efficient and precise markers and develop reliable models to predict pCR in ESCC patients undergoing NICT.

Radiomics is a method that utilizes algorithms to derive plenty of quantitative characteristics from images [13]. Computed tomography (CT) is a routine examination for tumor staging, and CT-based radiomics has been reported to assist in the noninvasive preselection for ESCC patient therapy [14]. Several previous studies [15, 16] modeled radiomics features based on pre-treatment CT for predicting pathological response to neoadjuvant chemotherapy or neoadjuvant chemoradiotherapy (NCRT) in esophageal cancer. Nonetheless, these researches were limited to a single period and did not include information about therapy responses.

Delta-radiomics is a novel concept that refers to changes in radiomics characteristics between initial and subsequent data throughout therapy. Some studies [17–19] have demonstrated the superiority of CT-based delta-radiomics for the prediction of response and prognosis to immunotherapy or chemotherapy for tumors such as lung, rectal, and gastric cancers. To date, there has been limited research on whether CT-based delta-radiomics can predict pCR to NICT in ESCC [20].

The study sought to explore the efficacy of CT-based delta-radiomics features in predicting pCR to NICT in ESCC patients. We hypothesize that these features can serve as reliable predictors of pCR, ultimately aiding clinicians in making optimal therapeutic decisions regarding altering the neoadjuvant treatment strategy or proceeding with surgery.

Materials

The study was conducted in accordance with the Declaration of Helsinki. This retrospective study was approved by the Ethics Committee of Wuhan Union Hospital, and the requirement for written informed consent was waived.

Patients and inclusion criteria

The study retrospectively included 140 ESCC patients from two institutions (Henan Provincial People's Hospital, Database 1 = 93; Wuhan Union Hospital, Database 2 = 47) who underwent NICT combined with surgery between June 1, 2020, and October 1, 2023. The following inclusion criteria were used: (1) age ≥ 18 years old; (2) in stage T1N1–3 or T2–4aN0–3 M0 by the eighth edition AJCC/UICC Tumor node metastasis (TNM) staging system [21]; (3) patients at least received two cycles of NICT;

(4) two contrast-enhanced CT scans, baseline CT and CT prior to the operation within one week, were obtained. Patients with missing data or CT images with artifacts were excluded from the analysis (Fig. 1). ESCC patients in our hospital are routinely given contrast-enhanced CT scans preoperatively, as these can provide detailed information on lesion morphology, enhancement characteristics, and boundary conditions, which are essential for staging and assessing therapeutic efficacy. Database 1 were allocated to the training set and Database 2 to the testing set. Additionally, we recorded the following clinical and radiographic characteristics of gender, age, body mass index (BMI), smoking status, drinking status, tumor location, tumor length, and cTNM. Tumor location was divided into upper, middle and lower esophagus according to the AJCC/UICC eighth edition [22]. BMI was derived from measurements of height and weight. The clinical TNM stage (cTNM) of ESCC was assessed using endoscopic ultrasound and enhanced CT.

To avoid including too many subjects, which could expose them to unnecessary risks and waste time and resources, or too few subjects, which might fail to achieve the desired objective, we calculated the sample size of the study using an online calculator [23] recommended by Monti et al. [24]. As shown in Supplementary 1, to estimate an AUC of 0.9 with a 95% confidence interval length of 0.15, given a sample prevalence of 30%, a total of 107 subjects would be required, indicating that our sample size was sufficient to support our results.

Treatment protocols

All patients underwent at least two cycles of NICT prior to surgery. The use of immune checkpoint inhibitors (ICIs) primarily involved pembrolizumab (200 mg), tislelizumab (200 mg), camrelizumab (200 mg), toripalimab (240 mg) or sintilimab (200 mg), administered intravenously every three weeks. The TP regimen incorporated platinum-based drugs (such as cisplatin or nedaplatin: 80 mg/m^2;carboplatin: AUC of 5 mg/ml/min) combined with paclitaxel (175 mg/m^2) or docetaxel (70 mg/m^2), administered intravenously every three weeks. The PF regimen included platinum-based drugs (50 mg/m^2) and 5-fluorouracil (800 mg/m^2 24 h by continuous infusion on days 1–4), given intravenously every two weeks. The dosage and administration of chemotherapeutic agents were tailored to each patient based on their individual condition and body surface area. ICIs are dosed using a fixed dose, depending on the specific drug. Surgery consisted of either open or minimally invasive transthoracic esophagectomy.

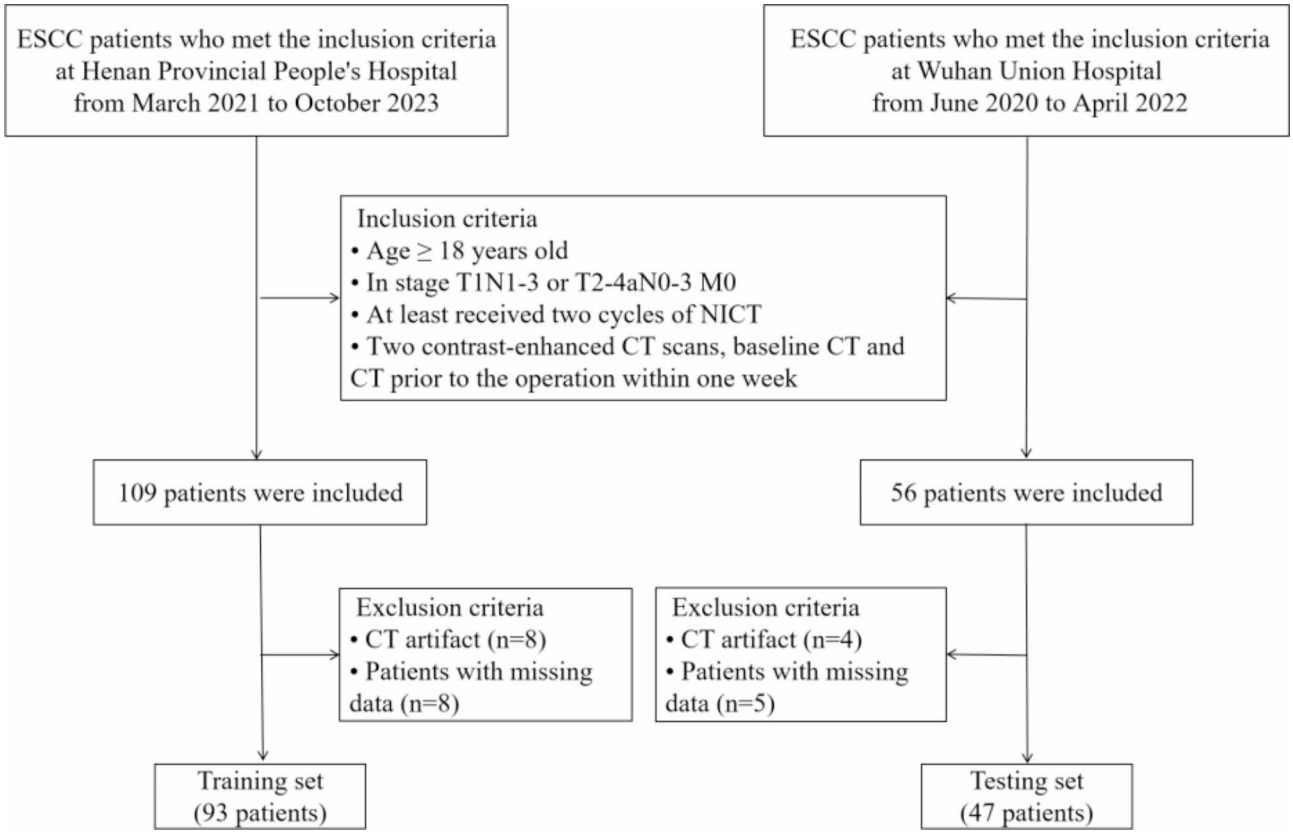

Fig. 1 Flow diagram shows patient selection and exclusion criteria. ESCC, esophageal squamous cell carcinoma; NICT, neoadjuvant immunochemotherapy; CT, computed tomography

Evaluation of tumor response

Similar to previous studies [16, 25], patients were categorized into two groups after NICT and surgery: the pCR group, composed of 40 patients, and the non-pCR group, composed of 100 patients, according to whether there were viable tumor cells in the primary tumor area and all resected lymph nodes.

CT image acquisition

Database 1 performed the CT scans using a multi-slice spiral CT scanner (GE Light Speed VCT). The acquisition settings were as follows: 64×0.6 mm collimation, automated tube current control at 120 kVp, reconstructed layer thickness and interval of 1.25 mm/1.25 mm. Nonionic iodine contrast medium (iopromide, Ultravist 300 mg/mL, Bayer, Germany) was injected intravenously at a 2.5–3.5 mL/s rate.

Database 2 performed the CT scans using two multi-slice spiral CT scanners (SOMATOM Definition, SOMATOM Definition AS+). The acquisition settings were as follows: 64×0.6 mm and 128×0.6 mm collimation, automated tube current control at 120 kVp, reconstructed layer thickness and interval of 1.5 mm/1.5 mm. Nonionic iodine contrast medium (iohexol 350 mg/mL, Beilu Pharmaceutical Co., Ltd.) was injected intravenously at a 2–3 mL/s rate.

Radiomics feature extraction

Two radiologists (HSS and YTZ, with 32 and 3 years of experience in thoracic radiology, respectively) semi-automatically delineated all cases on CT images using the 3D Slicer software without knowledge of the histologic findings. The tumor segmentation protocol was as follows [25, 26]: (1) delineate the tumor contour on the mediastinal (width, 350 HU; level, 40 HU) window of the contrast-enhanced CT images taken before and after NICT; (2) avoid the esophageal lumen during delineation; (3) the delineated region of interest (ROI) of the same patient remained consistent in position and length across both time points; (4) two radiologists evaluated all contours, and any disagreements regarding the tumor's boundaries must be resolved through discussion. The volumes of interest (VOIs) of tumors were automatically reconstructed using the 3D-slicer software. To minimize errors introduced by resampling, we analyzed the data to determine the most common voxel spacing, which was found to be (0.7, 0.7, 1.5) mm. Sixty-six of 140 (47.1%) 3D CT images were then resampled to this spacing using a B-spline curve interpolation algorithm. A bin width of 25 was applied for gray dispersion before radiomics examination. A total of 1037 radiomics features were extracted from the segmented ROI utilizing the Pyradiomics package in Python (Fig. 2, with additional details available at https://pyradiomics.readthedocs.io/en/latest/features. html) [27]. According to the image type, it can

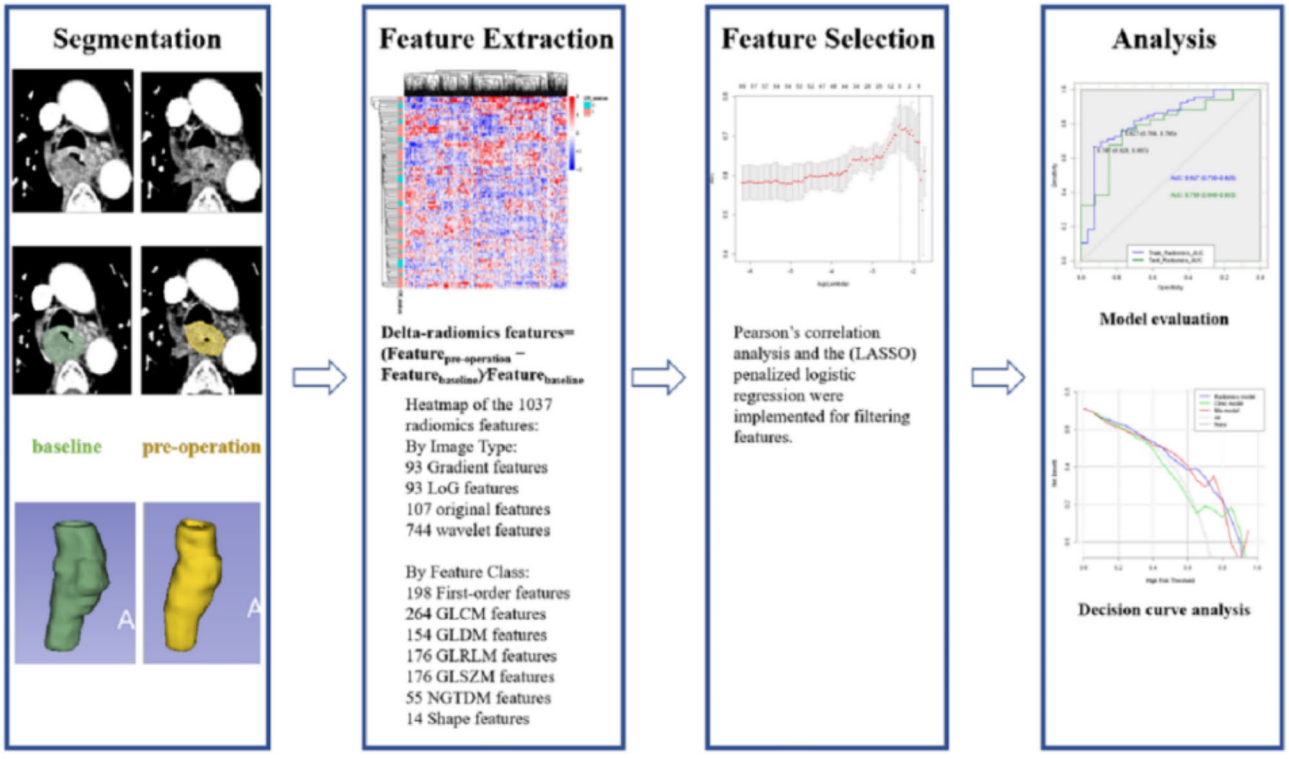

Fig. 2 Radiomics workflow

be classified into four types, including 93 gradient, 93 logarithmic transformed, 107 original, and 744 wavelet transformed features. Furthermore, based on the feature class, it can be categorized into 198 first-order features, 264 GLCM features, 154 GLDM features, 176 GLRLM features, 176 GLSZM features, 55 NGTDM features, and 14 shape features. Additionally, to assess intra-observer and inter-observer variability, we randomly selected 30 cases by using a random seed, and the intraclass correlation coefficient (ICC) was employed. Features with an ICC value exceeding 0.8 were considered to be stable and reproducible. Inter-observer repeatability was evaluated by two radiologists performing tumor segmentation on the same image collection, while intra-observer repeatability was assessed by one radiologist repeating segmentation one week later. SMOTE is used to generate artificial/synthetic samples for the minority class [28].

Delta-radiomics features

All patients underwent CT scans at baseline and prior to surgery. The radiomics features (RFs) were obtained at the two time points separately. The relative net change in RFs between these two time points is referred to as delta-RFs [29]:

Relative Net Change = $(\text{Feature}_{\text{pre-operation}} - \text{Feature}_{\text{baseline}})/\text{Feature}_{\text{baseline}}$.

Additionally, we conducted a self-assessment of our work using the CLEAR checklist [30] and METRICS score [31], which were included as Supplementary 2 and Supplementary 3, respectively.

Statistical analysis

The statistical analyses were conducted with SPSS 21 and R 4.0.2. Continuous variables were presented as mean±standard, and independent sample t tests were utilized for analysis. Categorical variables were presented as frequency (percentage), and analyzed using Fisher's exact test. Radiomics features were processed by z-score normalization. Pearson correlation analysis was used to eliminate the radiomics features with high correlation ($r>0.8$) in the training set. When two features exhibited a high correlation, we selected the feature with a stronger correlation to pCR, as indicated by a higher absolute Pearson correlation coefficient. And inter-observer variability analysis were employed to exclude features of low reliability (ICC<0.8). The fivefold cross-validation least absolute shrinkage and selection (LASSO) analysis was carried out for feature selection on the training set. A multivariate LR algorithm was used to build a classification model. Subsequently, four models were established: a clinical model, a pretreatment radiomics model, a delta-radiomics model, and a mixed model. Receiver operating characteristic (ROC) analysis was performed to evaluate the predictive performance of the models for pCR. The confounder matrix was used to demonstrate the predictive capacity of the models. The accuracy, sensitivity, and specificity of each model were then determined. The AUC values were utilized to express and compare the predictive performance of the models via the DeLong test. The two-tailed $p<0.05$ was considered statistically significant.

Results

Clinical and CT characteristics

In the study, most patients were male (108/140, 77.1%). The average age was 62.4±7.9 years, with a mean BMI of 23.2±3.2 kg/m^2. More than half of the participants were non-smokers (82/140, 58.6%) and non-drinkers (89/140, 63.6%). The majority of the tumors exhibited non-pCR (71.4%, 100/140, Fig. 3), and the rest of the tumors achieved pCR (28.6%, 40/140, Fig. 3). Most of the tumors were found in the middle esophagus (89/140, 63.6%). Regarding tumor staging, 67.1% of the patients (94/140) were diagnosed with stage III ESCC at baseline. The average tumor length was 70.9 mm (Table 1).

CT, computed tomography; ESCC, esophageal squamous cell carcinoma; NICT, neoadjuvant immunochemotherapy; pCR, pathological complete response.

The clinical model based on age and cTNM achieved good performance in predicting pCR in both the training and testing sets, yielding AUCs of 0.758 (95%CI, 0.658–0.858) and 0.615 (95%CI, 0.427–0.804), accuracy of 71% and 68.1%, specificity of 81.8% and 76.5%, and sensitivity of 44.4% and 46.1% (Fig. 4A, Table 2). The proportion of smokers, drinkers, and tumors located in the middle esophagus in the training set was notably higher than in the testing set. Besides, the training set exhibited greater age and tumor length in comparison to the testing set ($p<0.05$). Nevertheless, no significant differences were seen in sex, BMI, cTNM, or pCR ($p>0.05$) between the sets.

Pretreatment radiomics model

After eliminating 575 redundant and unstable features using Pearson correlation analysis and ICC, 462 radiomics features were selected for LASSO assessment. Subsequently, a pre-treatment radiomics model was established based on nine contributing radiomics features (Supplementary 4). The model achieved prediction performances for pCR of 0.787 (95%CI, 0.675-0.900) and 0.621 (95%CI, 0.436–0.806) in the training and testing sets, respectively, with the accuracy of 75.2% and 57.4%, specificity of 77.3% and 52.9%, and sensitivity of 70.4% and 69.2% in predicting pCR in the training and testing sets (Fig. 4B, Table 2).

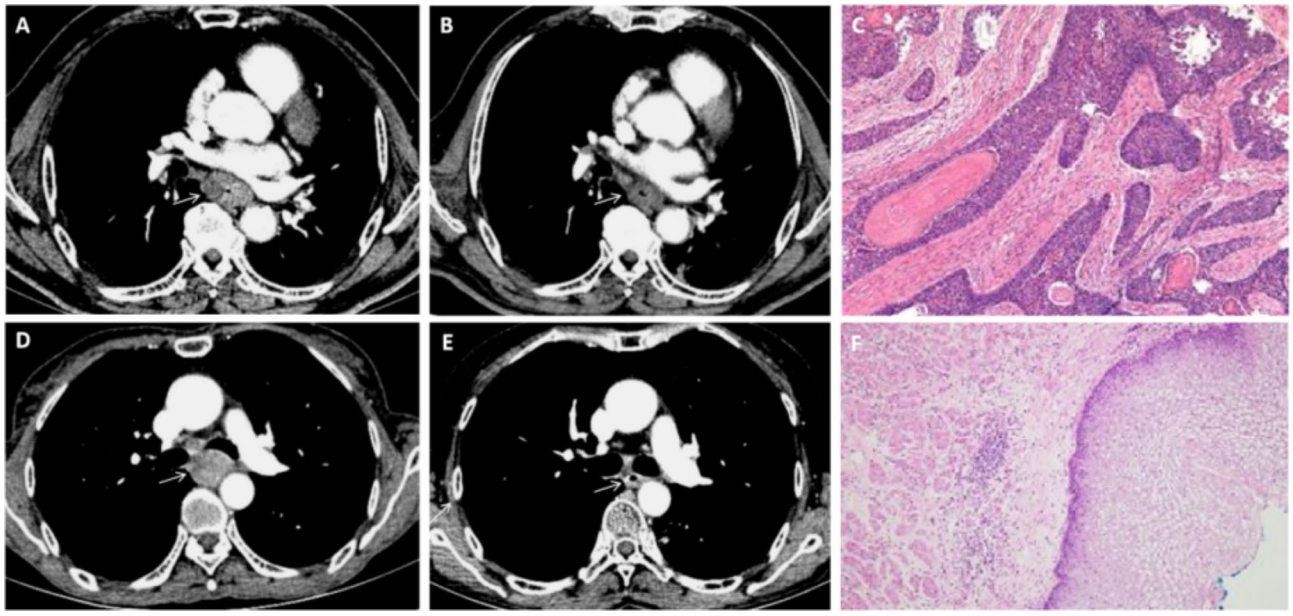

Fig. 3 Representative images of ESCC underwent NICT. (**A**, **B**) CT images of ESCC before and after NICT were shown (arrows). (**C**) Resection specimen showed this patient had non-pCR. (**D**, **E**) CT images of ESCC before and after NICT were shown (arrows). (**F**) Resection specimen showed this patient had pCR

Table 1 Demographic and clinical data of 140 cases from two institutions

Characteristic	Total patients ($n=140$)	Train ($n=93$)	Test ($n=47$)	*p* Value
Age (years)	62.4 ± 7.9	64.0 ± 8.0	59.2 ± 6.8	0.001*
Gender				0.291
Female	32 (22.9%)	24 (25.8%)	8 (17%)	
Male	108 (77.1%)	69 (74.2%)	39 (83%)	
BMI (kg/m^2)	23.2 ± 3.2	23.4 ± 3.2	22.8 ± 3.2	0.325
Smoking status				0.029*
Yes	58 (41.4%)	45 (48.4%)	13 (27.7%)	
No	82 (58.6%)	48 (51.6%)	34 (72.3%)	
Drinking status				0.026*
Yes	51 (36.4%)	40 (43%)	11 (23.4%)	
No	89 (63.6%)	53 (57%)	36 (76.6%)	
Tumor location				< 0.001*
Upper chest	15 (10.7%)	13 (14%)	2 (4.3%)	
Middle chest	89 (63.6%)	66 (71%)	23 (48.9%)	
Lower chest	36 (25.7%)	14 (15.1%)	22 (46.8%)	
Tumor length (mm)	70.9 ± 24.7	74.8 ± 24.3	63.1 ± 23.8	0.008*
TNM stage				0.296
II	36 (25.7%)	23 (24.7%)	13 (27.7%)	
III	94 (67.1%)	61 (65.6%)	33 (70.2%)	
IV	10 (7.1%)	9 (9.7%)	1 (2.1%)	
pCR				1
Yes	40 (28.6%)	27 (29%)	13 (27.7%)	
No	100 (71.4%)	66 (71%)	34 (72.3%)	

*$p<0.05$ based on comparisons between the two groups. Data are mean ± SD or n (%). BMI, body mass index; TNM, tumor node metastasis; pCR, pathological complete response

Delta-radiomics model

A total of 462 delta-radiomics features were identified for building the delta-radiomics model after conducting Pearson correlation analysis and ICC. It was found that five delta-radiomics features significantly differed between pCR and non-pCR tumors by using LASSO penalized logistic regression analysis (Fig. 5). The LR model recognized delta_wavelet.LLH_glrlm_Long

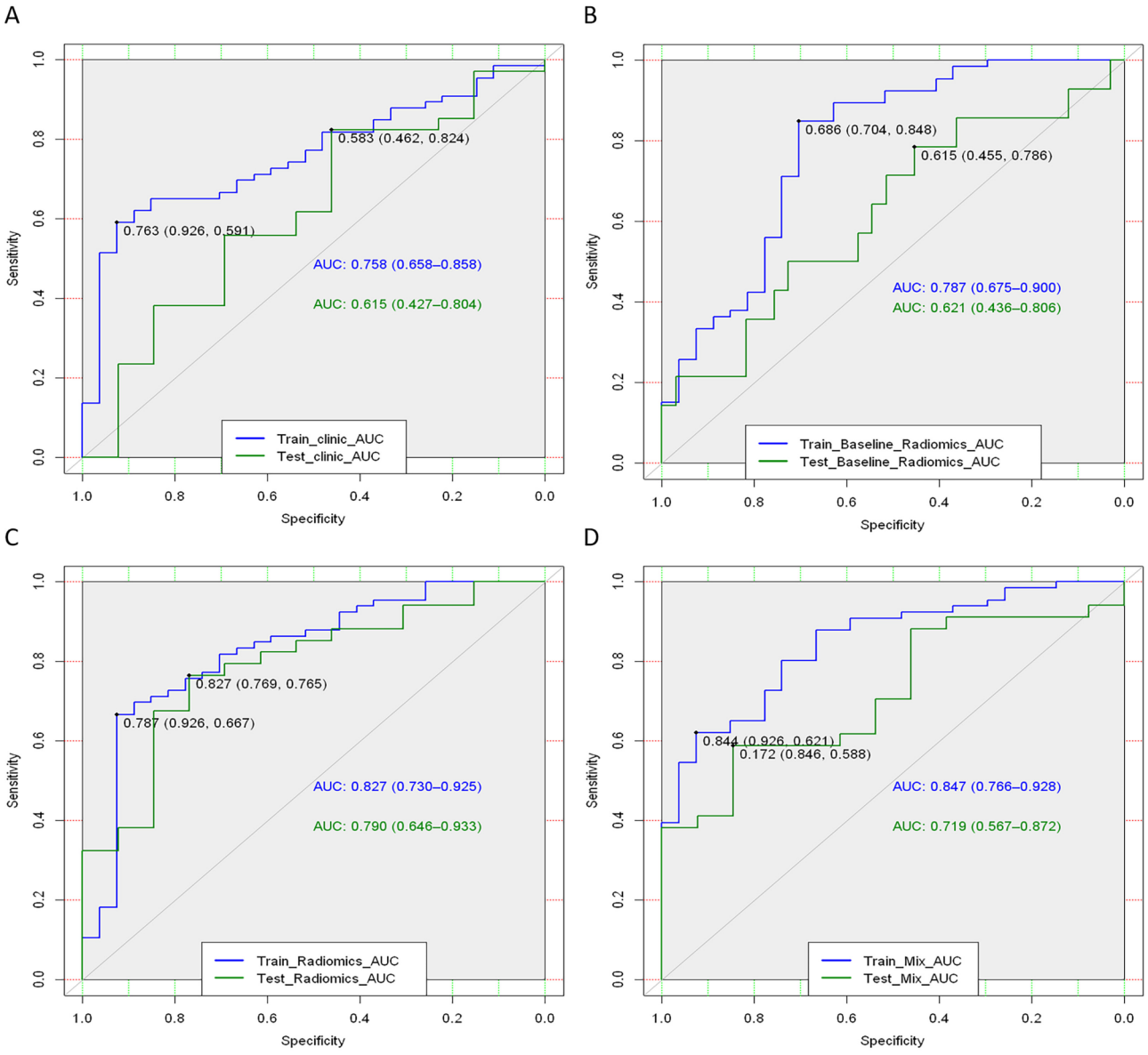

Fig. 4 Receiver operating characteristic curves for the prediction of pCR status of clinical model (**A**), pretreatment radiomics model (**B**), delta-radiomics model (**C**), and mixed model (**D**) in the training and testing sets. pCR, pathological complete response

RunLowGray Level Emphasis, delta_wavelet.LLL_gldm_ Small DependenceLowGray Level Emphasis, mean_ original_shape_SurfaceVolumeRatio, mean_wavelet. LHL_glcm_Idmn, and mean_ wavelet.HHL_firstorder_ Mean. A delta-radiomics model was then developed and achieved an AUC of 0.827 (95%CI, 0.730–0.925) in the training set and 0.790 (95%CI, 0.646–0.933) in the testing set. Table 3 presented the chosen delta-radiomics features and their corresponding coefficients. Moreover, the model achieved the accuracy of 74.2% and 72.3%, specificity of 68.2% and 70.6%, and sensitivity of 88.9% and 76.9% for pCR prediction in the training and testing sets (Fig. 4C, Table 2).

Mixed model

Additionally, we built a mixed model by incorporating selected clinical and delta-radiomics features. The model yielded an AUC of 0.847 (95%CI,0.766–0.928) in the training set and 0.719 (95%CI,0.567–0.872) in the testing set for predicting pCR (Fig. 4D). Moreover, the model demonstrated the accuracy of 71.0% and 61.7%, specificity of 68.2% and 52.9%, and sensitivity of 77.8% and 84.6% in the training and testing sets (Table 2). Subsequently, a nomogram consisting of age, cTNM, and Rad-score was built (Supplementary 5).

Table 2 Confounder matrix for the four sets in the four models

Predicted results	Actual results		AUC(95% CIs)	Accuracy (%)	Specificity (%)	Sensitivity (%)
	pCR	Non-pCR				
Clinical model						
Training data set			0.758[0.658–0.858]	71.0	81.8	44.4
pCR	12	12				
Non-pCR	15	54				
Testing data set			0.615[0.427–0.804]	68.1	76.5	46.1
pCR	6	8				
Non-pCR	7	26				
Pretreatment radiomics model						
Training data set			0.787[0.675-0.900]	75.2	77.3	70.4
pCR	19	15				
Non-pCR	8	51				
Testing data set			0.621 [0.436–0.806]	57.4	52.9	69.2
pCR	9	16				
Non-pCR	4	18				
Delta-radiomics model						
Training data set			0.827[0.730–0.925]	74.2	68.2	88.9
pCR	24	21				
Non-pCR	3	45				
Testing data set			0.790[0.646–0.933]	72.3	70.6	76.9
pCR	10	10				
Non-pCR	3	24				
Mixed model						
Training data set			0.847[0.766–0.928]	71.0	68.2	77.8
pCR	21	21				
Non-pCR	6	45				
Testing data set			0.719[0.567–0.872]	61.7	52.9	84.6
pCR	11	16				
Non-pCR	2	18				

pCR, pathological complete response; AUC, area under the curve; CI, confidence interval

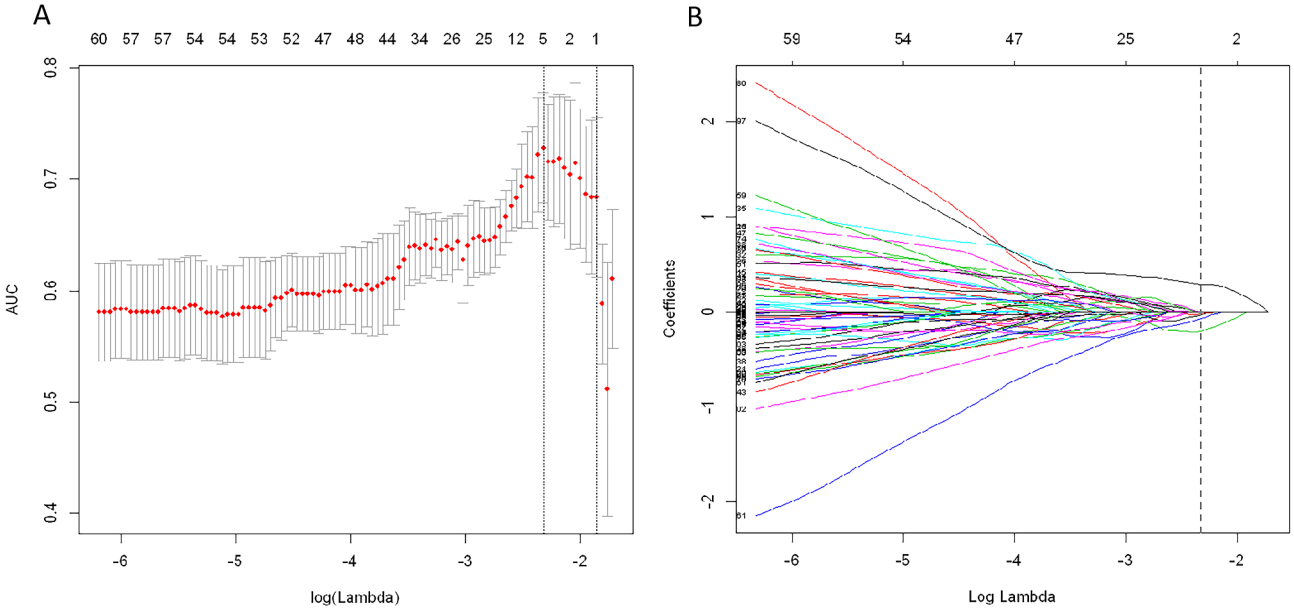

Fig. 5 Least absolute shrinkage and selection operator (LASSO) logistic regression of radiomics features (**A**) and the regularization parameterλ(**B**)

Table 3 Features included in the delta-radiomics model and their coefficients

	Estimate	Std. error	z value	Pr (>|z|)
(Intercept)	1.1253	0.2842	3.9591	0.0001
delta_wavelet.LLH_glrlm_LongRunLowGrayLevelEmphasis	-0.6926	0.2931	-2.3635	0.0181
delta_wavelet.LLL_gldm_SmallDependenceLowGrayLevelEmphasis	-0.4278	0.3398	-1.2589	0.2081
mean_original_shape_SurfaceVolumeRatio	-0.2071	0.3827	-0.5411	0.5884
mean_wavelet.LHL_glcm_Idmn	0.4298	0.3751	1.1457	0.2519
mean_wavelet.HHL_firstorder_Mean	-0.5306	0.3492	-1.5194	0.1287

Performance comparison between different models

The delta-radiomics model demonstrated a higher predictive ability in the testing cohort compared to the clinical, pre-treatment radiomics, and mixed models (AUC, 0.790 vs. 0.615 vs. 0.621 vs. 0.719, respectively). However, the differences in AUC values among the models were not statistically significant. Table 2 summarized the findings of confounder matrix analysis. The delta-radiomics model exhibited better accuracy, sensitivity, and specificity than the pretreatment radiomics model in the testing cohort.

Clinical use

Decision curve analysis (DCA) was conducted to assess the clinical utility of the prediction models (Fig. 6). Results showed that the clinical, pretreatment radiomics, delta-radiomics, and mixed models provided a positive net benefit for patients in comparison to the treat-all and treat-none models.

Discussion

Researches have demonstrated that pCR is related to improved prognosis, and predicting pCR can help make treatment decisions before surgery, assisting clinicians decide on the subsequent actions in the treatment plan, such as whether to modify the neoadjuvant treatment approach, proceed with surgery, or forgo surgery entirely. In the present study, a CT-based delta-radiomics model was built and validated for pCR prediction of NICT in ESCC patients, which performed well and was superior to the clinical, pretreatment radiomics and mixed models. This finding indicated that the delta-radiomics features can function as a crucial tool for decision assistance in identifying responses to NICT.

In our study, the average age of patients with ESCC was 62.4 years old, and approximately 77% of ESCC cases occurred in men, consistent with the standard population according to Global Cancer Statistics 2020 [2]. Conventional imaging can show features such as lesion size, location, and enhancement modalities but cannot reveal more in-depth information about ESCC. Some studies explored radiomics for predicting pathological response to ESCC. Oda et al. [15] developed a radiomics model based on pretreatment CT to predict pathological response to neoadjuvant chemotherapy for EC patients, achieving a sensitivity of 0.620, specificity of 0.860, and AUC of 0.815. Similarly, Wang et al. [16] used pretreatment CT-based radiomics features to predict the pathological response to NCRT in ESCC with an AUC of 0.817 in the testing set. However, these studies were limited to single time points and did not account for changes in therapy response.

In the study, the performance of the clinical and pretreatment radiomics models for predicting pCR to NICT was unsatisfactory, while the delta-radiomics model demonstrated strong performance, achieving an AUC of 0.827 and 0.790 in the training and testing sets, respectively. This may be because delta radiomics encompasses image- and time-dependent data and enables the dynamic evaluation of treatment-related tumor alterations. In addition, the mixed model combining clinical and radiomics features had a lower AUC value than the delta-radiomics model. The result may be that the inclusion of clinical features reduces the overall performance, suggesting that the delta-radiomics model is more robust.

According to the delta-radiomics model, five radiomics features were significantly correlated with response to NICT in ESCC patients. The SurfaceVolumeRatio refers to the mean of the surface area to volume ratio, suggesting that more compact and spherical profiles tend to have a better therapy response [32]. The firstorder_Mean indicated the mean gray level intensity within the tumor. The remaining three features were second-order features (glcm, gldm and glszm) that described the variability of gray-level intensity values in the image, thus reflecting the heterogeneity within the tumor [33]. The results indicated that the radiomics features, in addition to reflecting size and density, can also reveal heterogeneity of tumors, providing more information related to treatment response. Recent studies have shown that multi-omics approaches have the potential for improving cancer diagnosis and prognostic assessment [34–36]. Integrating radiomics with pathomics, metabolomics, and genomics can significantly enhance the predictive value compared to single-omics analyses. The role of this non-invasive method in esophageal cancer requires further exploration.

Furthermore, several studies revealed that therapy-induced changes in radiomics features may be valuable in predicting the prognosis of cancer patients [18, 29,

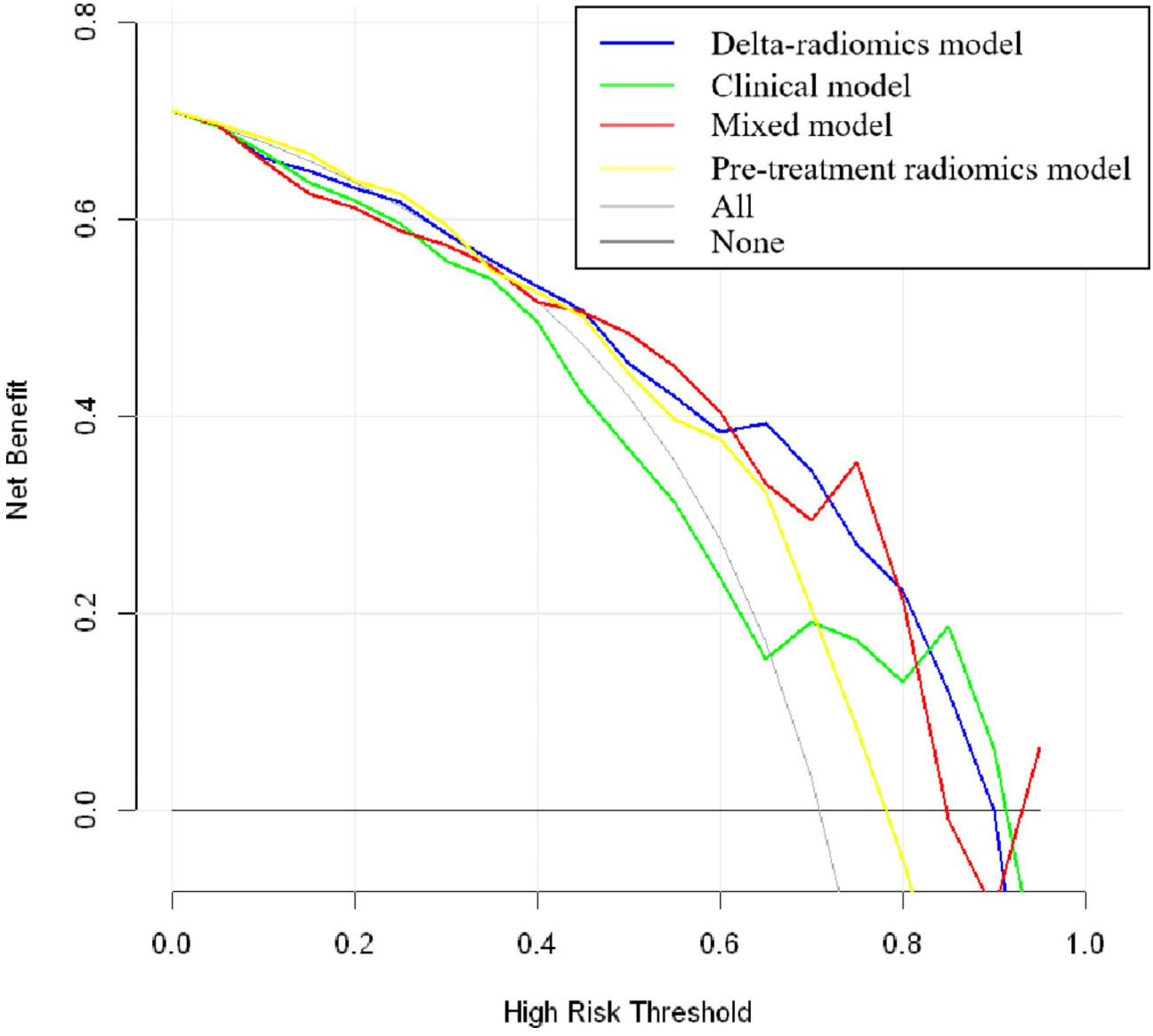

Fig. 6 Decision curve for the four models

37]. Shen et al. [18] demonstrated that CT-based delta-radiomics combined with preoperative clinical variables had a better prediction of prognosis after preoperative neoadjuvant chemotherapy in advanced gastric cancer than pathological TNM stage and tumor regression grade classification. Nakamoto et al. [37] attempted to evaluate the predictive value of delta-radiomics based on cone-beam CT for prognostic of patients with ESCC who received concurrent chemoradiotherapy. They revealed that there were significant differences in delta-radiomics features between the high- and low-risk groups, with a C-index value of 0.821. Thus, the value of delta-radiomics in predicting the prognosis of ESCC patients needs to be further investigated.

The research had certain limitations. Firstly, the retrospective nature and small sample size of the study could cause patient selection bias and poor generalization. Secondly, the difference in the CT scanning machines, imaging protocols and some demographic characteristics between the two databases may influence the results. However, we minimized these differences by resampling the CT images of the enrolled patients and normalizing the extracted radiomics features. The variability in multicenter radiomics studies should be addressed in the future. Thirdly, while SMOTE is effective at addressing class imbalance, it may also lead to overfitting and altering the data distribution, potentially reducing generalization performance and introducing bias. Fourthly, as there are no established or standardized guidelines for

esophageal cancer segmentation, the radiologists in our study followed protocols from prior research to perform tumor segmentation. Finally, no analysis was done on the correlation between biomarkers, such as PD-L1 expression, and radiomics features, because the study was retrospective.

Conclusions

In summary, we proposed a CT-based delta-radiomics model with promising performance in predicting pCR to NICT in ESCC patients, outperforming the clinical, pretreatment radiomics and mixed models. In the future, multicenter, multi-omics and large-scale studies need to be carried out to eliminate the flaws mentioned above and validate our findings. Additionally, exploring the connection between radiomics characteristics and cancer prognosis, as well as biomarkers, such as PD-L1 expression, can provide further insights.

Abbreviations

pCR	Pathological complete response
NICT	Neoadjuvant immunochemotherapy
ESCC	Esophageal squamous cell carcinoma
NCRT	Neoadjuvant chemoradiotherapy
CT	Computed tomography
TNM	Tumor node metastasis
BMI	Body mass index
ROI	Region of interest
ROC	Receiver operating characteristic
AUC	Area under the curve
ICC	Intraclass correlation coefficients
DCA	Decision curve analysis

Supplementary Information

The online version contains supplementary material available at https://doi.org/10.1186/s12880-024-01503-1.

Supplementary Material 1

Supplementary Material 2

Supplementary Material 3

Supplementary Material 4

Supplementary Material 5

Supplementary Material 6

Acknowledgements

Not applicable.

Author contributions

All authors contributed to the study conception and design. HSS, XYH, YDL and LW did the conception and design of the study.YTZ, PYM, MLW, QYL, HTL, KLZ, LQC and JG did the acquisition of data. CYD, YML, TTG, CZ and WJY did analysis and interpretation of the data. YTZ and PYM draft the article. All authors did final approval of the version to be submitted.

Funding

This study was supported by the National Natural Science Foundation of China (grant no.82071921, U22A20352) and Henan Province Medical Science and Technology Research Plan Provincial Ministry Key Project (No. SBGJ202302009).

Data availability

The data used and analyzed during the current study are available from the corresponding authors on reasonable request.

Declarations

Ethics approval and consent to participate

The study was conducted in accordance with the Declaration of Helsinki. This retrospective study was approved by the Ethics Committee of Wuhan Union Hospital, and the requirement for written informed consent was waived.

Consent for publication

Not applicable.

Competing interests

The authors declare no competing interests.

Clinical trial number

Not applicable.

Author details

[1]Department of Radiology, Union Hospital, Tongji Medical College, Huazhong University of Science and Technology, Wuhan 430022, China
[2]Hubei Province Key Laboratory of Molecular Imaging, Wuhan 430022, China
[3]Department of Thoracic Surgery, Union Hospital, Tongji Medical College, Huazhong University of Science and Technology, Wuhan 430022, China
[4]Department of Thoracic Surgery, Henan Provincial People's Hospital, People's Hospital of Zhengzhou University, School of Clinical Medicine, Henan University, Zhengzhou, Henan 450003, China
[5]Bayer Healthcare, No. 399, West Haiyang Road, Shanghai 200126, China

Received: 13 July 2024 / Accepted: 18 November 2024
Published online: 03 December 2024

References

1. Lagergren J, Smyth E, Cunningham D, Lagergren P. Oesophageal cancer. Lancet. 2017;390(10110):2383–96.
2. Sung H, Ferlay J, Siegel RL, Laversanne M, Soerjomataram I, Jemal A, et al. Global Cancer statistics 2020: GLOBOCAN estimates of incidence and Mortality Worldwide for 36 cancers in 185 countries. CA Cancer J Clin. 2021;71(3):209–49.
3. Uhlenhopp DJ, Then EO, Sunkara T, Gaduputi V. Epidemiology of esophageal cancer: update in global trends, etiology and risk factors. Clin J Gastroenterol. 2020;13(6):1010–21.
4. Ajani JA, D'Amico TA, Bentrem DJ, Chao J, Corvera C, Das P, et al. Esophageal and Esophagogastric Junction Cancers, Version 2.2019, NCCN Clinical Practice guidelines in Oncology. J Natl Compr Canc Netw. 2019;17(7):855–83.
5. Shapiro J, van Lanschot JJB, Hulshof MCCM, van Hagen P, van Berge Henegouwen MI, Wijnhoven BPL, et al. Neoadjuvant chemoradiotherapy plus surgery versus surgery alone for oesophageal or junctional cancer (CROSS): long-term results of a randomised controlled trial. Lancet Oncol. 2015;16(9):1090–8.
6. Sun JM, Shen L, Shah MA, Enzinger P, Adenis A, Doi T, et al. Pembrolizumab plus chemotherapy versus chemotherapy alone for first-line treatment of advanced oesophageal cancer (KEYNOTE–590): a randomised, placebo-controlled, phase 3 study. Lancet. 2021;398(10302):759–71.
7. Wu Z, Zheng Q, Chen H, Xiang J, Hu H, Li H, et al. Efficacy and safety of neoadjuvant chemotherapy and immunotherapy in locally resectable advanced esophageal squamous cell carcinoma. J Thorac Dis. 2021;13(6):3518–28.
8. Song XY, Liu J, Li HX, Cai XW, Li ZG, Su YC, et al. Enhancing prediction for Tumor Pathologic response to Neoadjuvant Immunochemotherapy in locally Advanced Esophageal Cancer by dynamic parameters from clinical assessments. Cancers (Basel). 2023;15(17):4377.
9. Yang Y, Tan L, Hu J, Li Y, Mao Y, Tian Z, et al. Esophageal Cancer Committee of Chinese Anti-cancer Association. Safety and efficacy of neoadjuvant treatment with immune checkpoint inhibitors in esophageal cancer: real-world multicenter retrospective study in China. Dis Esophagus. 2022;35(11):doac031.

10. Yang Y, Xin D, Wang H, Guan L, Meng X, Lu T, et al. A novel predictor of pathologic complete response for Neoadjuvant Immunochemotherapy in Resectable locally advanced esophageal squamous cell carcinoma. J Inflamm Res. 2023;16:1443–55.
11. Wang X, Yang W, Zhou Q, Luo H, Chen W, Yeung SJ, et al. The role of 18F-FDG PET/CT in predicting the pathological response to neoadjuvant PD–1 blockade in combination with chemotherapy for resectable esophageal squamous cell carcinoma. Eur J Nucl Med Mol Imaging. 2022;49(12):4241–51.
12. Feng J, Wang L, Yang X, Chen Q, Cheng X. Prediction of pathologic complete response prediction in patients with locally advanced esophageal squamous cell carcinoma treated with neoadjuvant immunochemotherapy: a real-world study. Biomol Biomed. 2023;23(1):153–60.
13. Lambin P, Leijenaar RTH, Deist TM, Peerlings J, de Jong EEC, van Timmeren J, et al. Radiomics: the bridge between medical imaging and personalized medicine. Nat Rev Clin Oncol. 2017;14(12):749–62.
14. Zhu Y, Yao W, Xu BC, Lei YY, Guo QK, Liu LZ, et al. Predicting response to immunotherapy plus chemotherapy in patients with esophageal squamous cell carcinoma using non-invasive radiomic biomarkers. BMC Cancer. 2021;21(1):1167.
15. Oda S, Kuno H, Hiyama T, Sakashita S, Sasaki T, Kobayashi T. Computed tomography-based radiomic analysis for predicting pathological response and prognosis after neoadjuvant chemotherapy in patients with locally advanced esophageal cancer. Abdom Radiol (NY). 2023;48(8):2503–13.
16. Wang J, Zhu X, Zeng J, Liu C, Shen W, Sun X, et al. Using clinical and radiomic feature-based machine learning models to predict pathological complete response in patients with esophageal squamous cell carcinoma receiving neoadjuvant chemoradiation. Eur Radiol. 2023;33(12):8554–63.
17. Gong J, Bao X, Wang T, Liu J, Peng W, Shi J, et al. A short-term follow-up CT based radiomics approach to predict response to immunotherapy in advanced non-small-cell lung cancer. Oncoimmunology. 2022;11(1):2028962.
18. Shen LL, Zheng HL, Ding FH, Lu J, Chen QY, Xu BB, et al. Delta computed tomography radiomics features-based nomogram predicts long-term efficacy after neoadjuvant chemotherapy in advanced gastric cancer. Radiol Med. 2023;128(4):402–14.
19. Giannini V, Pusceddu L, Defeudis A, Nicoletti G, Cappello G, Mazzetti S, et al. Delta-Radiomics predicts response to First-Line oxaliplatin-based chemotherapy in Colorectal Cancer patients with Liver metastases. Cancers (Basel). 2022;14(1):241.
20. Ruan Y, Ma Y, Ma M, Liu C, Su D, Guan X, et al. Dynamic radiological features predict pathological response after neoadjuvant immunochemotherapy in esophageal squamous cell carcinoma. J Transl Med. 2024;22(1):471.
21. Rice TW, Ishwaran H, Blackstone EH, Hofstetter WL, Kelsen DP, Apperson-Hansen C. Worldwide Esophageal Cancer collaboration investigators. Recommendations for clinical staging (cTNM) of cancer of the esophagus and esophagogastric junction for the 8th edition AJCC/UICC staging manuals. Dis Esophagus. 2016;29(8):913–9.
22. Rice TW, Ishwaran H, Ferguson MK, Blackstone EH, Goldstraw P. Cancer of the Esophagus and Esophagogastric Junction: an Eighth Edition staging primer. J Thorac Oncol. 2017;12(1):36–42.
23. Sample size- confdence interval for AUROC | Sample Size Calculators. https://sample-size.net/sample-size-ci-for-auroc/. Accessed 10 Feb 2024.
24. Monti CB, Ambrogi F, Sardanelli F. Sample size calculation for data reliability and diagnostic performance: a go-to review. Eur Radiol Exp. 2024;8(1):79.
25. Yang Y, Yi Y, Wang Z, Li S, Zhang B, Sang Z, et al. A combined nomogram based on radiomics and hematology to predict the pathological complete response of neoadjuvant immunochemotherapy in esophageal squamous cell carcinoma. BMC Cancer. 2024;24(1):460.
26. Li K, Li Y, Wang Z, Huang C, Sun S, Liu X, et al. Delta-radiomics based on CT predicts pathologic complete response in ESCC treated with neoadjuvant immunochemotherapy and surgery. Front Oncol. 2023;13:1131883.
27. van Griethuysen JJM, Fedorov A, Parmar C, Hosny A, Aucoin N, Narayan V, et al. Computational Radiomics System to Decode the Radiographic phenotype. Cancer Res. 2017;77(21):e104–7.
28. Chawla NV, Bowyer KW, O.Hall L, Kegelmeyer WP. SMOTE: synthetic minority over-sampling technique. J Artif Intell Res. 2002; 321–57.
29. Fave X, Zhang L, Yang J, Mackin D, Balter P, Gomez D, et al. Delta-radiomics features for the prediction of patient outcomes in non-small cell lung cancer. Sci Rep. 2017;7(1):588.
30. Kocak B, Baessler B, Bakas S, Cuocolo R, Fedorov A, Maier-Hein L, et al. CheckList for EvaluAtion of Radiomics research (CLEAR): a step-by-step reporting guideline for authors and reviewers endorsed by ESR and EuSoMII. Insights Imaging. 2023;14(1):75.
31. Kocak B, Akinci D'Antonoli T, Mercaldo N, et al. METhodological RadiomICs score (METRICS):a quality scoring tool for radiomics research endorsed by EuSoMII. Insights Imaging. 2024;15(1):8.
32. Caruso D, Polici M, Rinzivillo M, Zerunian M, Nacci I, Marasco M, et al. CT-based radiomics for prediction of therapeutic response to Everolimus in metastatic neuroendocrine tumors. Radiol Med. 2022;127(7):691–701.
33. Li Y, Wang B, Wen L, Li H, He F, Wu J, et al. Machine learning and radiomics for the prediction of multidrug resistance in cavitary pulmonary tuberculosis: a multicentre study. Eur Radiol. 2023;33(1):391–400.
34. Cicalini I, Chiarelli AM, Chiacchiaretta P, Perpetuini D, Rosa C, Mastrodicasa D, et al. Multi-omics staging of locally advanced rectal cancer predicts treatment response: a pilot study. Radiol Med. 2024;129(5):712–26.
35. Li L, Duan J, Gao Y, Yin Y, Yang F, Tang W, et al. Multi-omics predictive model based on clinical, radiomic and genomic features for predicting the response of limited-stage small cell lung cancer to definitive chemoradiotherapy. Clin Transl Med. 2024;14(1):e1522.
36. Su GH, Xiao Y, You C, Zheng RC, Zhao S, Sun SY, et al. Radiogenomic-based multiomic analysis reveals imaging intratumor heterogeneity phenotypes and therapeutic targets. Sci Adv. 2023;9(40):eadf0837.
37. Nakamoto T, Yamashita H, Jinnouchi H, Nawa K, Imae T, Takenaka S, et al. Cone-beam computed-tomography-based delta-radiomic analysis for investigating prognostic power for esophageal squamous cell cancer patients undergoing concurrent chemoradiotherapy. Phys Med. 2024;117:103182.

Publisher's note